Heat transfer Augmentation in Double Pipe Heat Exchanger by Using (Al_2O_3) Nano-fluid

تحسين أنتقال الحرارة داخل مبادل حراري مزدوج الأنبوب باستخدام المائع النانوي أوكسيد الالمنيوم (Al_2O_3)

Dr. Mohammed W. Al-Jibory[1], Ahmad Sabah Al-hilaly [2]
1 Ph.D., Lec.,Kerbala Univ., Mech. Eng. Dept., maljibory71@yahoo.com, dr.mohammed.wahab@uokerbala.edu.iq..
2 Mechanical Engineer, ahmedsabah121992@gmail.com.

Abstract:

In this study, the turbulent flow and heat transfer characteristics of Al_2O_3/Distilled water Nano-fluid with a range of the Reynolds number (Re = 6196.92–38669.54) and the range of volume concentrations (φ =0.5%, 1%, and 2%) are concentrated tentatively and numerically. The test rig includes cold liquid circle, hot liquid circle and the test portion, which is counter stream dual pipe heat exchanger with (2000) mm length. The chilly fluid (Distilled water) flowing through the external tube and the hot fluid (or Nano-liquid) move through the inner tube. The limit conditions of numerical (CFD) study is the same conditions as in experimental work additionally, thermally protected of the external wall. The hot Nano-liquid loop side with uniform speed at (0.176, 0.352, 0.529, 0.705, 0.881 and 1.058) m/s, and the cold distilled water circle with constant speed of (0.529) m/s. The outcomes were demonstrated that, the warmth transfer coefficient, (Nusselt numbers) expanded by expanding, Reynolds number, and the molecular concentration. The experimental and Numerical results indicate that the maximum enhancement in heat transfer coefficient (Nusselt number) were (48.93) % and (46.63) % separately, and the increasing in the friction factor was about (7.69) % as compared to the distilled water at the maximum discharging of (18) Liter/min and volume concentration of (2) %. Theoretical study included numerical analysis to solve governing differential equations in three dimensions through use of ready-program workbench ANSYS FLUENT bundle-(16) to study the effect of both Reynold number and focus on the amount of improvement in heat transfer and friction variable. The test results were demonstrated a decent concurrence with numerical results with the minimum and maximum difference were (5.75 and 11.41) percentage and the normal difference was (10.074) percentage was happening with Distilled-water.

Keywords: Nusselt number, Al_2O_3 Nano-fluid, heat exchanger.

الخلاصة:

في هذا البحث، تم إجراء دراسة عملية وعددية لانتقال الحرارة لجريان اضطرابي كامل التشكل داخل مبادل حراري مزدوج الانبوب. باستخدام نوع واحد من أنواع الموائع متناهية الدقة لأكاسيد معدنية هو، [(γ-Al_2O_3 (20 nm)) - distilled water] وبتراكيز حجمية مختلفة (φ = 0%, 0.5%, 1%, 2%) ومدى عدد رينولد للجريان الأضطرابي (Re = 6196.92-38669.54)، الجانب العملي من الدراسة تضمن بناء منظومة اختبار تحتوي على أجهزة القياس والآلات الضرورية لحساب مقدار التحسين في انتقال الحرارة , حيث ان الظروف النظرية كانت مشابهة الى الظروف العملية حيث كانت السرع للمائع الحار في الانبوب الداخلي للمبادل كالتالي (0.176 , 0.352, 0.529, 0.705, 0.881, 1.058) متر/ثانية و السرعة ثابتة للأنبوب الخارجي مقدارها (0.529) متر/ثانية.

أظهرت النتائج ان تحسين انتقال الحرارة يرتبط بزيادة التركيز الحجمي للجزئيات متناهية الصغر وكذلك مدى رينولد. وتم الحصول على أفضل نسبه في انتقال الحرارة للنتائج العملية والعددية عن طريق نسبه عدد نسلت والتي بلغت %(48.93) و % (46.63) من خلال (Al_2O_3) مع الماء وان الزيادة في معامل الاحتكاك للمائع النانوي بلغت %(7.69) من الماء عند اعلى تصريف (18 لتر/دقيقة) وتركيز (φ=2%)على التوالي.

تضمن الدراسة النظرية التحليل العددي باستخدام تقنية الحجوم المحددة لحل المعادلات التفاضلية الحاكمة بالأبعاد الثلاثة

من خلال استخدام البرنامج الجاهز (workbench ANSYS FLUENT bundle-16) لدراسة تأثير كل من عدد رينولد والتركيز على مقدار التحسين في انتقال الحرارة ومعامل الاحتكاك.
من خلال إجراء المقارنة بين النتائج العملية والنظرية لوحظ تطابق جيد بين النتائج وبأقل وبأعلى نسبه اختلاف % (5.75 و11.41) ومعدل اختلاف %(10.074) كانت عند استخدام المائع المتناهي الدقة (Al_2O_3) وبتركيز (φ =2%).

1. Introduction

Fast advancement in all sectors, which is foundations, modern, transportation, defense, space overseeing high heat loads has turned out to be extremely basic. For that reason, several cooling technologies have been researched. However, the conventional technique of heat transfer by means of a flow system including fluids like water, ethylene glycol, mineral oils has always been popular and would always remain popular due to its simple nature. Conventional heat transfer systems used in applications like petrochemical, refining, and power generation are rather large and involve significant amount of heat transfer. However, in certain applications like electronics cooling in laptops and microprocessors, engine cooling in automobiles, cooling in power electronics used in military devices, cooling in space applications and many other areas, small heat transfer systems are required. These applications have a critical relationship between size of a mechanical system and the cost associated with manufacturing and operation. If improvements could be made in the existing heat transfer systems such as enhancing the performance of the heat transfer fluid, a lesser heat exchanger surface area and hence, a lesser space would be required to handle a specified amount of cooling load. The situation would lead to smaller heat transfer systems with lower capital costs and higher energy efficiencies. In this pursuit, numerous researchers have been investigating better techniques to enhance the thermal performance of heat transfer fluids. One of the methods used is to add Nano-sized particles of highly thermally conductive materials like carbon, metal, metal oxides into the heat transfer fluid to improve the overall thermal conductivity of the fluid. The dispersion or suspension thus obtained is called Nano-fluid [1].

Numerous researchers have contemplated the heat transfer qualities of the different Nano-fluids. Concentrating on the constrained of forced convective heat transfer experimentally, a few existing distributed articles that include the utilization of Nano-fluids are talked about in the subsequent sections.

Pak and Cho, [2] concentrated tentatively the heat transfer of (Al_2O_3-water) Nano-liquid at turbulent stream when point of interest of heat exchanger and the limit conditions were round tube ($D = 10.66$) mm and length ($L = 4.8$) m at steady warmth flux. At scope of Reynolds number ($Re = 10^4 - 10^5$)and particle concentration (φ): 1.34%, 2.78% and 4.33% by volume. From the results were found that the Nusselt number of the scattered liquids for completely created stream increased by increasing volume concentration and in addition with Reynolds number. Additionally found that the extreme upgrade of heat transfer coefficient, was 12% littlest than, that in unadulterated water with 3% particle concentration.

Fotukian and Esfahany, [3] concentrated tentatively, the turbulent stream of Nano-liquid with various volume concentrations (φ = 0.03%, 0.054%, 0.067% and 0.135%) by volume of (γ-Al_2O_3) nanoparticles. The Nano-liquid was streaming at steady wall temperatures with the scope of Reynolds number about from (6×10^4 to 3.1×10^4), through shell and tube heat exchanger consist of the inner diameter of the tube equal to (d_i=5 mm) and the shell inner diameter equal to (D_i=32 mm). Results had obviously demonstrated the increasing in, the proportion of heat transfer coefficient for Nano-liquid with Reynolds number, contrasted with immaculate water by (48 %) with the high volume concentration (φ=0.054%).

Vasu et al., [4] built up an exact relationship for thermal conductivity of ($\mathrm{Cu/water}$) and ($\mathrm{Al_2O_3/water}$) Nano-liquids, considering the impacts of temperature, volume portion, and size of the nano molecule. A relationship for the evaluation of, Nusselt number was additionally, developed, displayed, and looked at, in graphical appearance. Those relationships improved thermo-physical and heat exchange characteristics made liquids embedded with nano-materials as brilliant candidates for future applications.

Eiamsa-Ardet al., [5] studied experimentally the influence of CuO/water Nano-fluid with the particles concentrations that utilize were (φ=0.3%, 0.5% and 0.7%) by volume and corrugated tube equipped with twisted-tape with twist ratio equal to (y/w=2.7) on the thermal performance. The (CuO) Nano-fluid was streaming, through the steel concentric tube heat exchanger consist of the inner diameter of inner tube equal to (d_i=10 mm) and the shell internal diameter equivalent to (D_i=25 mm), and the extent of Reynolds number about from (6.2×10^3 to 24×10^3) in addition to, the maximum thermal performance factor of (1.57) was found in counter arrangements at turn proportion of (y/w=2.7) and Reynolds number of (6.2 x 103), with volume concentration (φ=0.7%).

Khalifa and Banwan, [6] studied experimentally the effect of (γ-Al_2O_3/water) Nano-fluids with various volume concentrations (φ=0.25%, 0.5%, 0.75% and 1%) by volume on warmth transfer under turbulent regime (Re $\geq$ 2300) in in counter double pipe heat exchanger concentric tube for four diverse mass stream rates about (2.5, 3.333, 4.166 and 5) Liter/min, and the temperature for hot water was (50) ^oC. The dimensional for the test rig has the inner diameter of internal pipe (d_i=20 mm) with thickness 1mm and shell inner diameter equal to (D_i=50 mm) and thickness (2mm), and length (L=760mm) in additional to, the Results exhibited the convective warmth transfer increase by extending volume concentration and stream rate. The most extreme improvement got for Nusselt number and the warmth transfer coefficient were (20 and 22.8) percentage, separately, at Reynolds number (6026) and particle concentration was (φ=1) percentage.

Nguyen et al., [7] studied experimentally the examination on turbulent warmth transfer in closed system for cooling chip with (Al_2O_3/water)Nano-liquids at molecule concentrations were (φ= 1 %, 3.1 % and 6.8 %) by volume. The Reynolds numbers extend that used as a part of this study from (3×10^3 to 15×10^3). He reasoned that the consideration of nanoparticles into water created an impressive upgrade of the cooling piece convective warmth transfer coefficient. Results demonstrated the most extreme improvement in warmth transfer coefficient was 40% at molecule concentration (φ=6.8%).

Vajjha et al., [8] investigated experimentally the heat transfer of (Al_2O_3, SiO_2 and Cuo) Nano-fluid at turbulent flow(Re $\geq$ 2300). The detail of heat exchanger and the boundary conditions was circular pipe (D=314mm) and length (L=1168 mm) at consistent heat flux. The field of Reynolds numbers, which used from (Re= 3000 to 16000), and the molecule concentrations were (φ=2%, 4%, 6%, 8% and 10%) by volume. The all outcomes were exhibited that by expanding the molecule concentration, the result lead to the pressure drop (friction factor)and warmth transfer rates increase also it demonstrated the greatest improvement of heat transfer coefficient was 81.74% at molecule concentration (φ = 10%) and (Re = 7.24×10^3).

Heydar et al., [9] concentrated tentatively the examined of heat transfer for Titanium dioxide nanoparticles (TiO_2/ water)Nano-fluid at turbulent flow (Re $\geq$ 2300). The detail of the test section (double tube heat exchanger) and the boundary conditions was inner pipe diameter(d_i = 6 mm) and shell inner diameter (D_i=14 mm) with length (L=120cm) at constant temperature of Nano-fluid (T=35 and 40) Celsius. The range of Reynolds number (Re) that used about (10×10^3– 27.5×10^3), the particle concentration 0.01%, by volume with and without twist-tape has ratio equal to (y=3.5). By using twisted-tape with titanium oxide Nano-fluid, the efficiency 30percentage as compared to the base and about 10% without using the twist tape.

2. Experimental Apparatus

Operational segment was carried out in heat transfer laboratory in the college of engineering, university of Karbala, as shown in figures (1 and 2), the test section is a double pipe heat exchanger and it is constructed from concentric copper tube with (2000 mm) length. The copper tube with inner diameter is (19 mm), and outer diameter is (22 mm), was chosen as the inner tube. In addition to, the shell, side consists of a Poly vinyl Chlorid (PVC) tube with inner diameter (52 mm) and outer diameter is (63 mm), was chosen as the outer tube for the test section. The hot fluid flows in the inner tube while the cooling fluid flows in the annulus.

Where the working fluids of the inner cycle were [Distilled-water, and metal oxide Nano-fluid type Aluminum Oxide Nano-fluid (Al_2O_3)] with volume concentrations of (φ = 0.5, 1 and 2) percentage. The flow consists of the hot fluid tank, heater, pump, flow meter, two control valves and a piping system. The hot fluid tank is made of Plate, which has a volume capacity (50) liters and used to feed the system with the required amount of hot fluid through the pump and collect the accumulated fluid comes from the test section. U-tube manometer was used to measure the pressure drop across the inner tube of heat exchanger. The power of heater was (3000) Watt. The circulating pump is a centrifugal pump [TAAM - 220 V - 50 Hz - 0.37 kW], [Qmax = 30 L/min, Hmax = 30 m] used for circulating the hot fluid, through the experimental test rig. The two pumps for shell (cold-water side) is a centrifugal pump of type [MARQUIS - 220 V - 50 Hz – 2900 RPM], [Qmax = 30 L/min, Hmax = 30 m], and the other [SUPER - 220 V - 50 Hz – 2850 RPM], [Qmax = 60 L/min, Hmax = 50 m]. The flow meters with a range, (2 – 18 L/min) was used to measure the flow rate of the hot fluid in the inner tube and shell side with error (±0.033 L/min).

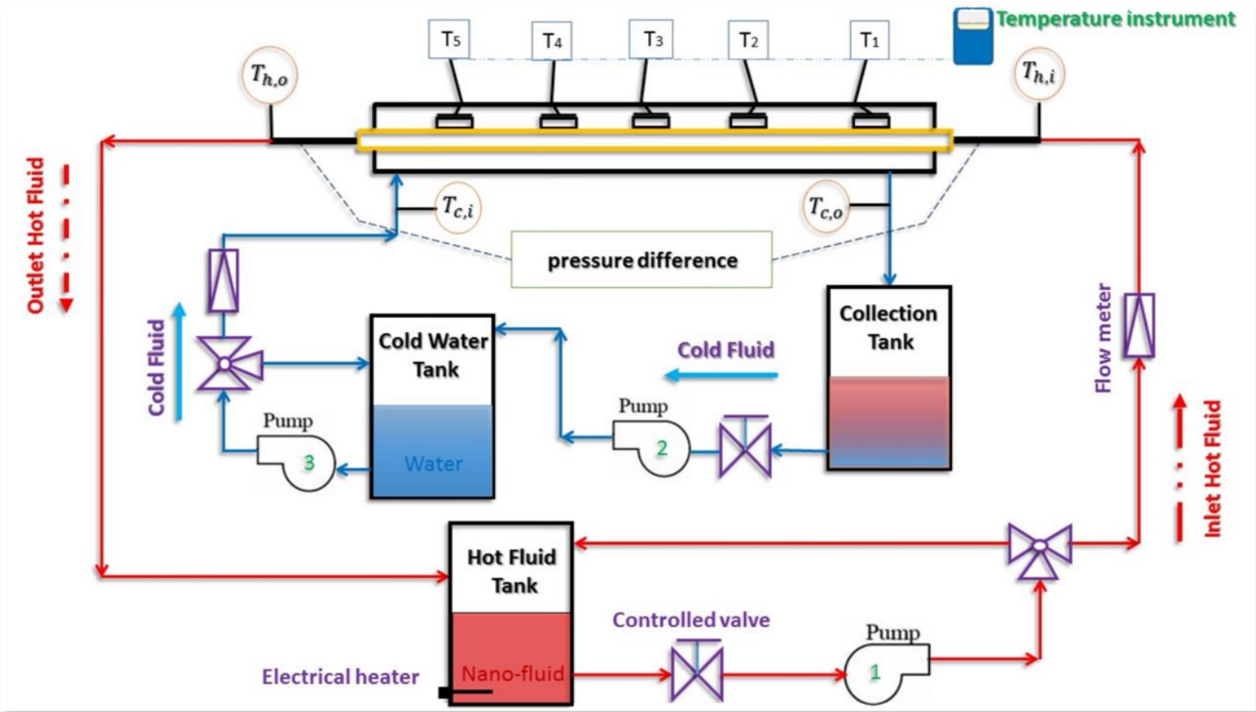

Figure (1): Schematic diagram of experimental apparatus.

Nine thermocouples (K–type) were used to measure the temperature in different locations along the test rig of heat exchanger. Five thermocouples were used to measure the temperatures along the outer surface of the inner tube at the heated test section. The thermocouples are located along the test section with a space distance of (350) mm between each other. The thermocouples were fixed on the specified place with epoxy adhesion. Four thermocouples were immersed in the working fluid in order to measure the inlet, and the outlet temperature for the hot, and cold fluids (shell and tube) sides of the test section. The thermocouples were calibrated at the Center of Standardization and Quality Control with error (± 1.1) C^{o}.

Figure (2): Experimental apparatus.

3. Data Reduction

a) Thermo-physical Properties of Nano-Fluid

The physical-properties for the Nano-fluid used for this work are by compared the measuring properties at 20 C^{o} and then selection the suitable equation to calculate physical properties at the film temperature of Nano-fluid by using the standard equations [10]**,** and the nanoparticles physical properties are shown in table (1).

The Thermal Conductivity of Nano-fluid (k_{nf}) in W/m.K is determined by the following equation:

$$k_{nf} = \left[\frac{k_p+2k_w+2(k_p-k_w)(1+\beta)^3\varphi}{k_p+2k_w-(k_p-k_w)(1+\beta)^3\varphi}\right]k_w \qquad .... (1)$$

The Dynamic viscosity of Nano-fluid (μ_{nf}) in pa.sec is determined by the following equation:

$$\mu_{nf} = \left[\frac{1}{(1-\varphi)^{2.5}}\right]\mu_w \qquad .... (2)$$

The specific heat Nano-fluid (Cp_{nf}) in kJ/kg.K is determined by the following equation:

$$Cp_{nf} = \frac{(1-\varphi)Cp_{bf}\rho_{bf}+\varphi\,\rho_p Cp_p}{\rho_{nf}} \qquad .... (3)$$

The density Nano-fluid (ρ_{nf}) in kg/m³ is determined by the following equation:

$$\rho_{nf} = (1-\varphi)\rho_{bf} + \varphi\rho_p \qquad .... (4)$$

b) Mathematical Calculations

In the present study, the γ-Al_2O_3 nanoparticles dispersed in distilled-water were used to investigate the convective heat transfer coefficient and Nusselt number of the Nano-fluid. Thus, it can be calculated from the following equations:

The amount of the heat transferred from the geyser heater to the working fluid (heat absorbed) is given by:

1- The heat transfer rate through tube (hot side)

$$Q_{Nano-fluid} = \dot{m}_{nf} \times C_{nf} \times (T_o - T_i)_{nf} \quad \text{…. (5)}$$

2- The heat transfer rate through shell side (cold side)

$$Q_{Water} = \dot{m}_{w} \times C_{w} \times (T_o - T_i)_{w} \quad \text{…. (6)}$$

3- Heat Transfer Coefficient (Nusselt Number)

Experimentally, the heat transfer coefficient can be calculated from Newton's law of cooling such as [11]:

$$Q_{Nano-fluid} = h_i A_s (T_{wall} - T_{Mean}) \quad \text{…. (7)}$$

$$h_i = \frac{Q_{Nano-fluid}}{A_s\,(T_{wall} - T_{mean})} \quad \text{…. (8)}$$

$$\mathrm{Nu_i} = \frac{h_i\, d_i}{\mathrm{K}} \quad \text{…. (9)}$$

Where;
The surface area of the inner tube

$$A_s = \pi \times d_i \times L \quad \text{…. (10)}$$

The surface mean wall temperature of the inner tube

$$T_{wall} = \frac{T_1 + T_2 + T_3 + T_4 + T_5}{5} \quad \text{…. (11)}$$

The bulk temperature at the inlet and outlet of the inner tube

$$T_b = \frac{T_{h,i} + T_{h,o}}{2} \quad \text{…. (12)}$$

4- Reynolds Number and Entrance Length

The Reynolds number (Re) of cooling water and hot Nano-fluid are obtained by the following equations:

$$\mathrm{Re} = \frac{\rho\, w\, d}{\mu} \quad \text{…. (13)}$$

Or,

$$\mathrm{Re} = \frac{4\,\dot{m}}{\pi\, d\mu} \quad \text{…. (14)}$$

The entrance length to ensure the flow is hydrodynamic fully developed was obtained by the following equations[12]:

$$\mathrm{Re} = \left(\frac{\mathrm{L_e}}{4.4 \times \mathrm{d_i}}\right)^6 \quad \text{…. (15)}$$

5- Friction Factor

The friction factor can be calculated by using the expression of Darcy equation[13].

$$f = \frac{2\,\Delta P d_i}{\rho w^2 L} \qquad \text{…. (16)}$$

Where;

$$\Delta \mathrm{P} = \rho g \Delta H \qquad \text{…. (17)}$$

c) Governing Equations

The basic equations that describe the flow and heat by using Ansys-16- FLUENT in 3D are conservation of momentum, mass, and energy equations. These, equations numerically describe three-dimensional, turbulent and incompressible flow takes which the following forms [14] .

The assumptions that used for the instantaneous equation are:-

1- Steady, three-dimensional, incompressible flow, single-phase flow, no-slip, irrotational.

2- Thermal-equilibriums between the nano-particles, and base liquid.

(i) Conservation of Mass:

$$\frac{\partial \rho}{\partial t} + \frac{\partial u}{\partial x} + \frac{\partial v}{\partial y} + \frac{\partial w}{\partial z} = 0 \qquad \text{….(18)}$$

(ii) Momentum Equations:

a) Momentum equation in the X-direction:

$$\frac{\partial \rho u}{\partial t} + \frac{\partial(\rho u u)}{\partial x} + \frac{\partial(\rho v u)}{\partial y} + \frac{\partial(\rho w u)}{\partial z} = -\frac{\partial p}{\partial x} + \rho g_x + \mu\left[\frac{\partial^2 u}{\partial x^2} + \frac{\partial^2 u}{\partial y^2} + \frac{\partial^2 u}{\partial z^2}\right] \qquad \text{... (19)}$$

b) Momentum equation in the Y-direction:

$$\frac{\partial \rho v}{\partial t} + \frac{\partial(\rho u v)}{\partial x} + \frac{\partial(\rho v v)}{\partial y} + \frac{\partial(\rho w v)}{\partial z} = -\frac{\partial p}{\partial y} + \rho g_y + \mu\left[\frac{\partial^2 v}{\partial x^2} + \frac{\partial^2 v}{\partial y^2} + \frac{\partial^2 v}{\partial z^2}\right] \qquad \text{... (20)}$$

c) Momentum equation in the Z-direction:

$$\frac{\partial \rho w}{\partial t}+\frac{\partial(\rho u w)}{\partial x}+\frac{\partial(\rho v w)}{\partial y}+\frac{\partial(\rho w w)}{\partial z}=-\frac{\partial p}{\partial z}+\rho g_z+\mu\left[\frac{\partial^2 w}{\partial x^2}+\frac{\partial^2 w}{\partial y^2}+\frac{\partial^2 w}{\partial z^2}\right] \quad ...(21)$$

(iii) Energy Equation

$$\frac{\partial}{\partial x}\left(\rho u h-\Gamma\frac{\partial h}{\partial x}\right)+\frac{\partial}{\partial y}\left(\rho v h-\Gamma\frac{\partial h}{\partial y}\right)+\frac{\partial}{\partial z}\left(\rho w h-\Gamma\frac{\partial h}{\partial z}\right)=0 \quad \ldots (22)$$

Where;

$$\Gamma = \mu/\Pr \quad \ldots. (23)$$

(iv) Turbulence Model

The turbulence model that utilized in this analysis is one of the most widely used turbulence models is the two-equation model of kinetic energy (k) and its dissipation rate (ε)[15].

(i) Turbulence Energy, (k)

$$\frac{\partial \rho k}{\partial t}+\frac{\partial}{\partial x_i}(\rho k u_i)=\frac{\partial}{\partial x_j}\left[\left(\mu+\frac{\mu_t}{\sigma_k}\right)\frac{\partial k}{\partial x_j}\right]+G_k-\rho\varepsilon \quad \ldots. (24)$$

(ii) Energy Dissipation Rate, (ε)

$$\frac{\partial \rho \varepsilon}{\partial t}+\frac{\partial}{\partial x_i}(\rho \varepsilon u_i)=\frac{\partial}{\partial x_j}\left[\left(\mu+\frac{\mu_t}{\sigma_\varepsilon}\right)\frac{\partial \varepsilon}{\partial x_j}\right]+\left(\rho C_{1\varepsilon}\frac{\varepsilon}{k}G_k\right)-\left(\rho C_{2\varepsilon}\frac{\varepsilon^2}{k}\right) \quad \ldots. (25)$$

Where;

The turbulent (or eddy) viscosity,(μ_t)

$$\mu_t=\rho C_\mu\frac{k^2}{\varepsilon} \quad \ldots. (26)$$

Also, the generation of turbulence kinetic energy due to the mean velocity gradients ($\mathbf{G_k}$),

$$G_k=\mu_t\, S^2 \quad \ldots. (27)$$

S: is the modulus of the mean rate-of-strain tensor, defined as

$$S=\sqrt{S_{ij}S_{ij}} \quad \ldots.(28)$$

$$S_{ij}=\frac{1}{2}\left(\frac{\partial u_j}{\partial x_i}+\frac{\partial u_i}{\partial x_j}\right) \quad \ldots.(29)$$

The model constants have the following default values[16], as shown in table (2) .

4. Boundary Condition and Number of Iteration

Boundary conditions for temperatures, pressure, velocities, and parts of the double pipe heat exchanger were defined in table (3). In additional to, the error of residual data set is (10^{-3} and 10^{-6}) for continuity, (κ- ε) model, velocities and energy respectively, are satisfied, the solution said, to be converging, as shown in figure (3) of the scaled Residuals.

Typically, about (170-300) iterations are needed to obtain a converged result, which takes about (2 to 6) hours for each case, on a computer a cluster consisting of (2.60) GHz, Processer Intel® CORE (TM) i7, memory (6) GB personal computers.

5. Results and Discussion

Figure (4) displays the Nusselt number against the Reynolds number and the results of this validation are in a good agreement between the numerical data and the data from the correlation equation of Dittos–Boelter with the minimum difference (8.98) percentage and the maximum difference (12.64) percentage and the normal difference (10.66) percentage of the Nusselt number.

Figure (5) displays the friction factor number against the Reynolds number of distilled water, the results showed good agreement between the results obtained by the numerical data with the empirical correlation equation, of Blasius with the maximum difference (4.17) percentage and the normal difference (2.033) percentage of the friction factor.

The comparison between the experimental and numerical results are shown in figures (6) for the distilled-water. A good agreement between the results are noticed, the minimum and maximum difference were (5.75 and 11.41) percentage and the average difference was (10.074) percentage of all the data sets.

Figure (7) shows the variation of the experimental Nusselt number with Reynolds number for (Al_2O_3) Nano-fluid at an inlet constant temperature was (50) °C for three values of volume concentrations (φ= 0.5,1 and 2) percentage. It shows that as Reynolds number increases, the Nusselt number increases too in all cases. The high Nuselt number was obtained with concentration of (2) %. The enhancement in the heat transfer (Nusselt number) between the maximum and minimum values of volume concentrations of Al_2O_3 Nano-fluid is explained using the Nusselt number percentage are (21.02) % and (16.29) % when the discharging was (18 and 3) L/min respectively. The results of Nusselt number and the uncertainty error for all data sets are shown in table (4 and 5) respectively.

Figure (8) represents the relation between experimental friction factor and Reynolds number for the smooth tube heat exchanger. The increase in the pressure drop (friction factor) for a friction factor ratio was ($f_{\text{Nano-fluid}}/f_{\text{Distilled-water}}$). The minimum and maximum increasing in the friction factor for friction factor ratio ($f_{Al2O3}/f_{\text{Distilled-water}}$) of ($Al_2O_3$) Nano-fluid with volume concentrations (0.5 and 2) % were (1.044) and (1.0769), which occurred with the maximum discharging was (18) L/min respectively. From the outcomes which appeared, the friction factor of (Al_2O_3) Nano-fluid with all volume concentrations are higher than Distilled-water because of the changing in fluid properties (high viscosity) lead to increase the values of the friction factor as shown in the same figure.

Figures (9) display contours of temperature distribution across the shell and tube in Kelvin (K) at locations of (Z= 30, 65, 100, 135, 170, 200) cm along the test section for volume concentration (φ=2) percentage of (Al_2O_3) Nano-fluid. The inlet temperature of the hot Nano-fluid equal to (50) ^oC, and the cold-water temperature was equal to (18.6) ^oC, when the discharging was (9) L/min for both side of working fluids. Notice that include difference temperature contours of (Al_2O_3) Nano-fluid between the sections to another for the inner tube because of the cooling that happen by the cold water in shell side on inner tube.

Figure (10) shows a focused view of the temperature contours along the anterior section (Z-axis), of the heat exchanger for the hot Nano-fluid and cold-water. The temperature at an inlet for the hot Nano-fluid equals to (50) ^oC and the discharging was (18) L/min. The cold-water temperature was equal to (18.6) ^{o}C at the inlet, and the discharging was (9) L/min. With volume concentration (φ=2) % of (Al_2O_3) Nano-fluid.

6. Conclusions

1. Experimentally, by using aluminum dioxide (Al_2O_3) Nano-fluid with the volume concentrations of (0.5, 1 and 2) percentage in the double pipe heat exchanger lead to improve the heat transfer coefficient (Nusselt number) about (23.1, 39, and 48.93) percentage at maximum flow rate respectively, as compared to the distilled water.
2. The maximum volume concentration of (2) percentage with using aluminum dioxide (Al_2O_3) Nano-fluid lead to increase the friction factor about (7.69) percentage as compared to the base fluid.
3. The change in fluid properties with increasing of volume concentrations (φ=0.5, 1and 2) percentage, and increasing Reynolds number this lead to improvement in the heat transfer (Nusselt number).
4. Results show that the experimental data sets are in good agreement with the numerical data related to Nusselt number for distilled water and the observed uncertainty error is low for all cases in this study, as shown in table (4).

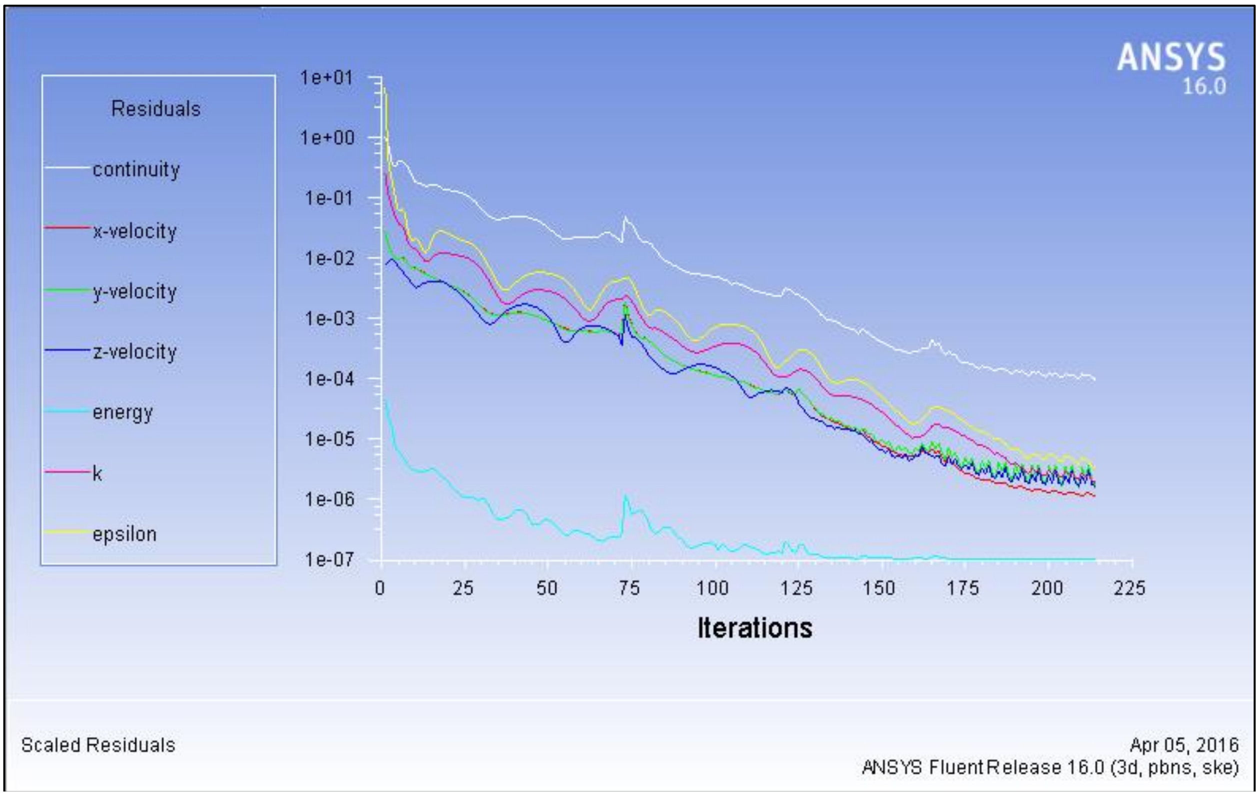

Figure (3): Scaled Residuals

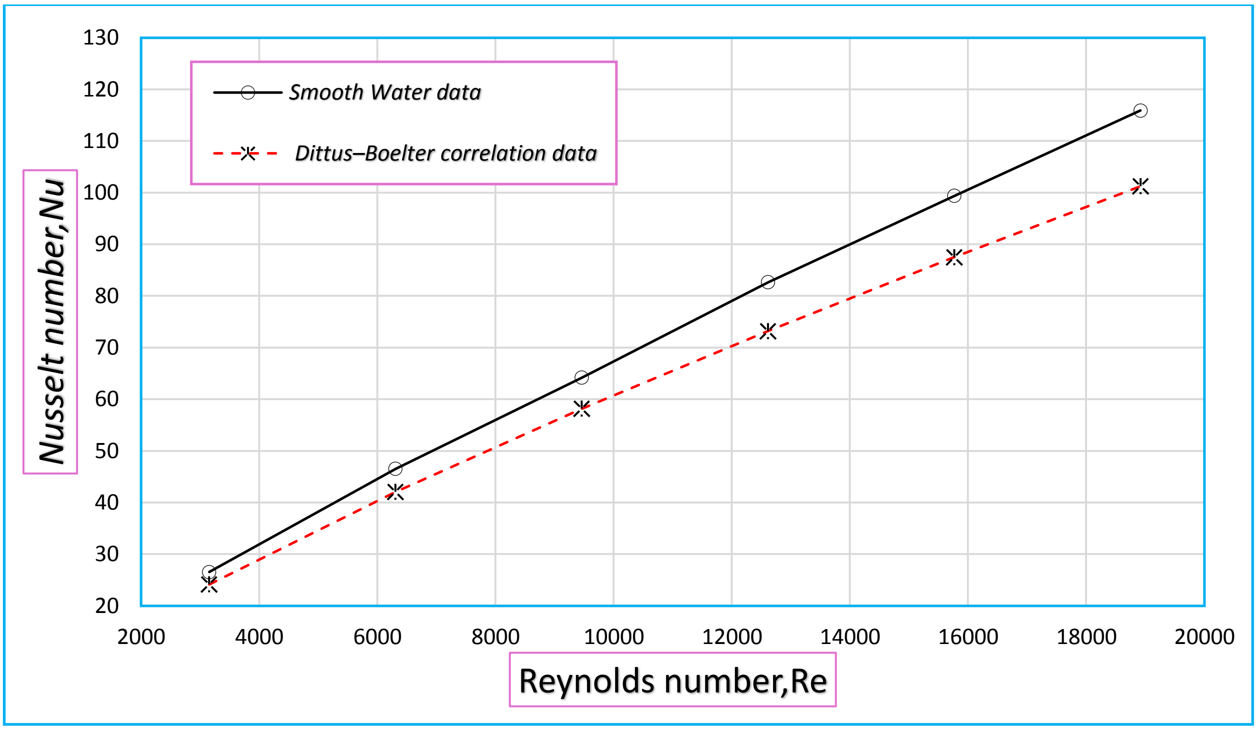

Figure (4) : Comparison between Numerical Nusselt numbers of distilled water with correlation of Dittos–Boelter.

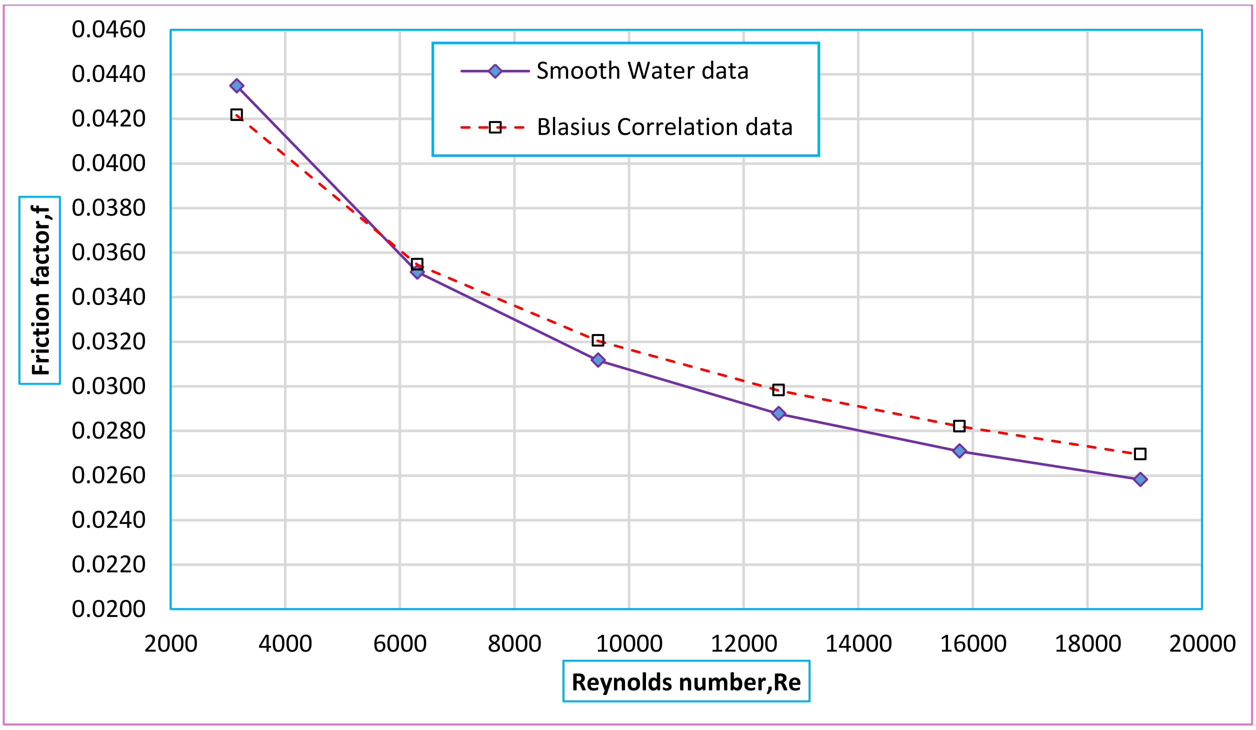

Figure (5): Numerical Friction factor of distilled water in comparison with correlation of Blasius.

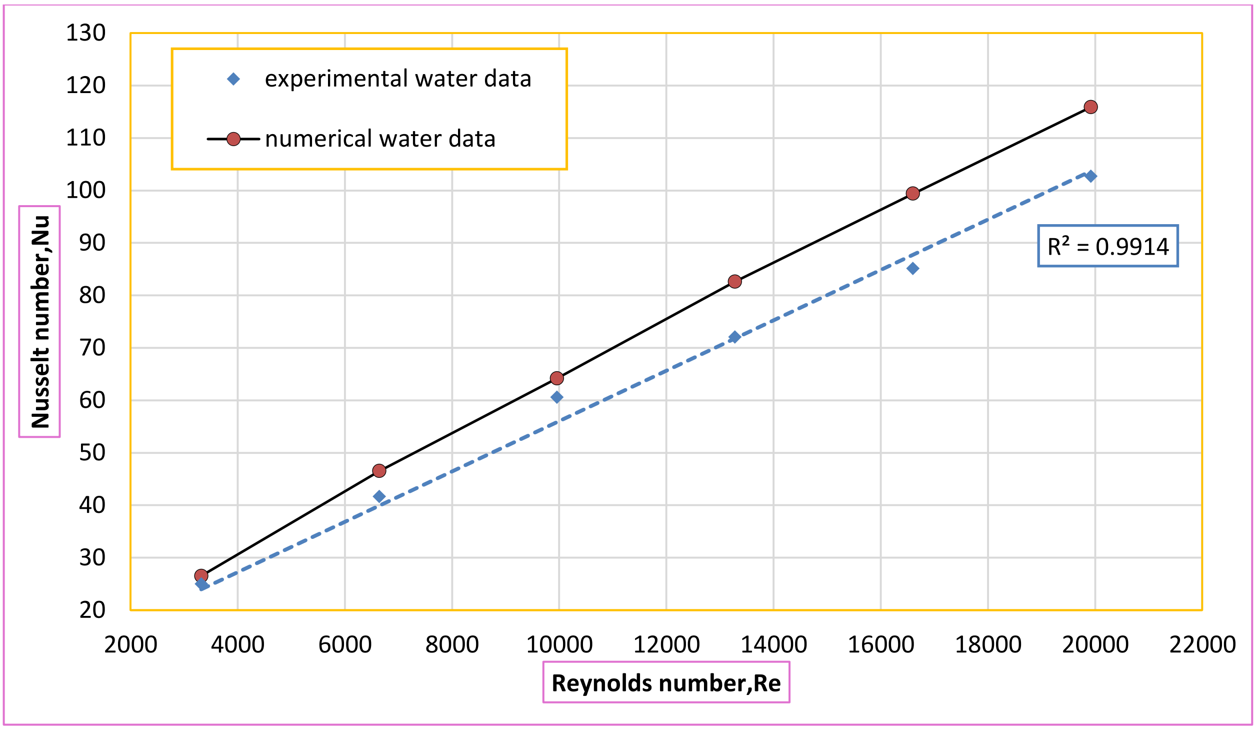

Figure (6): Numerical Nusselt number of distilled water in comparison with experimental data.

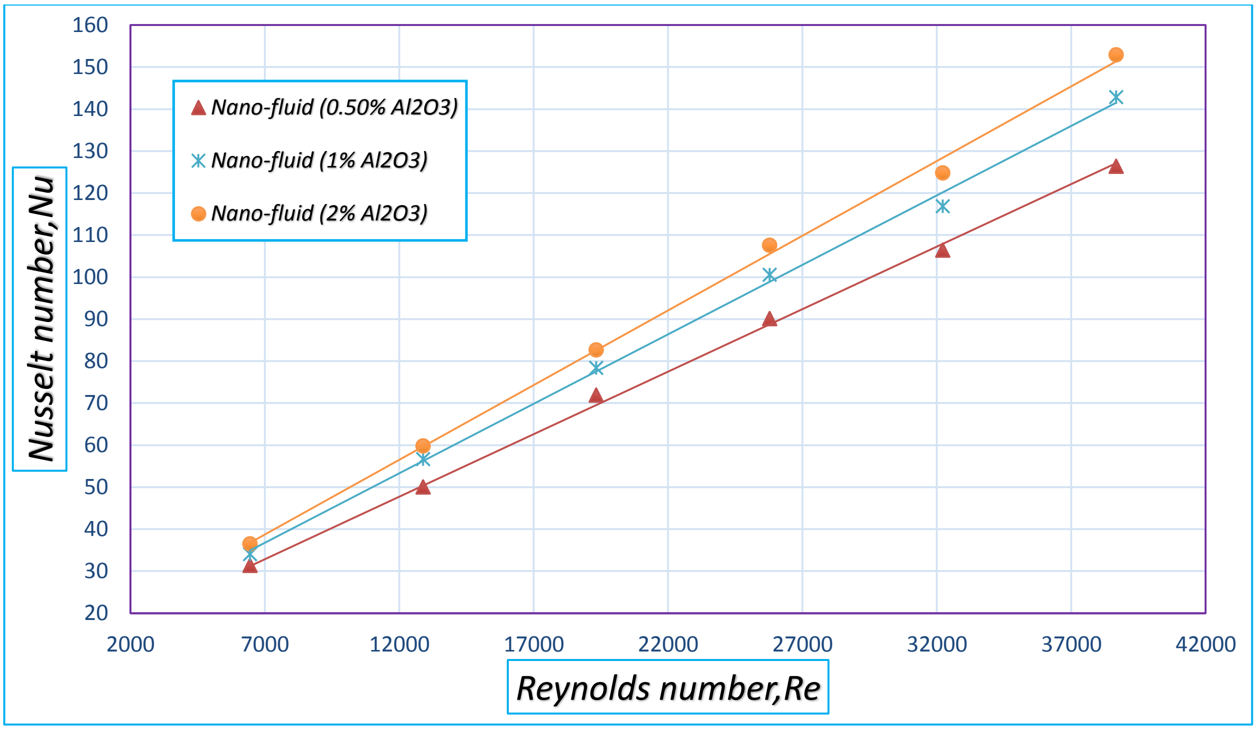

Figure (7): The effect of volume concentration of (Al_2O_3) Nano-fluid on Nusselt number at different Reynolds number.

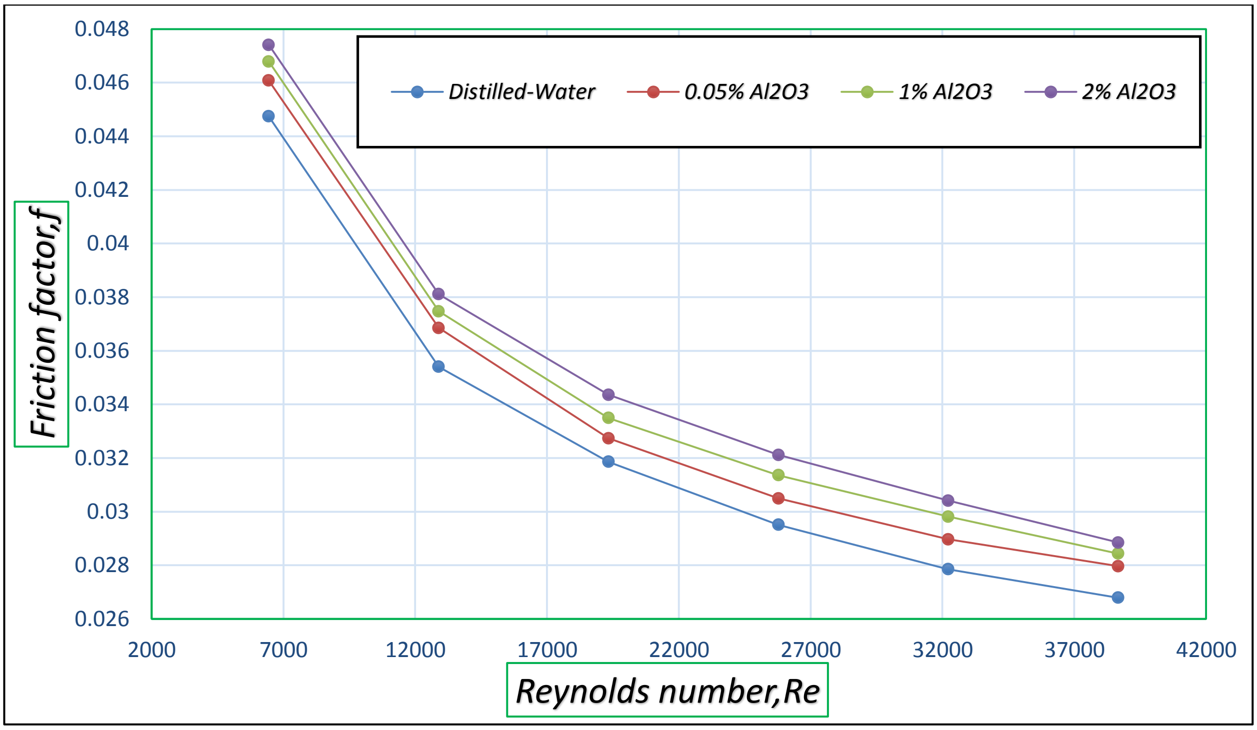

Figure (8): The effect of volume concentration of (Al_2O_3) Nano-fluid on friction factor at different Reynolds number.

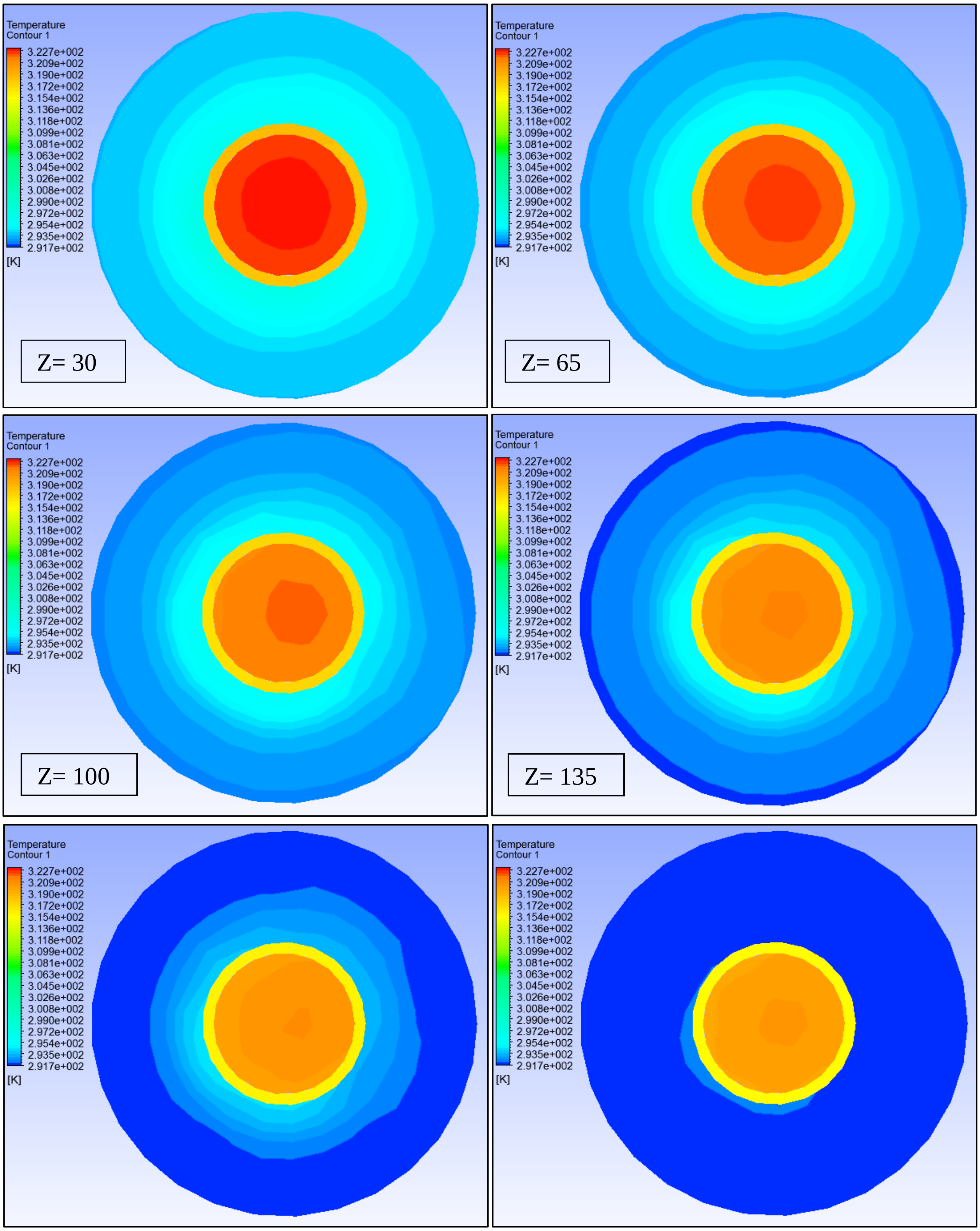

Figure (9): Temperature contours in (K) at locations of (Z= 30, 65, 100, 135, 170, 200) cm along the test section for Nano-fluid [2% Al_2O_3].

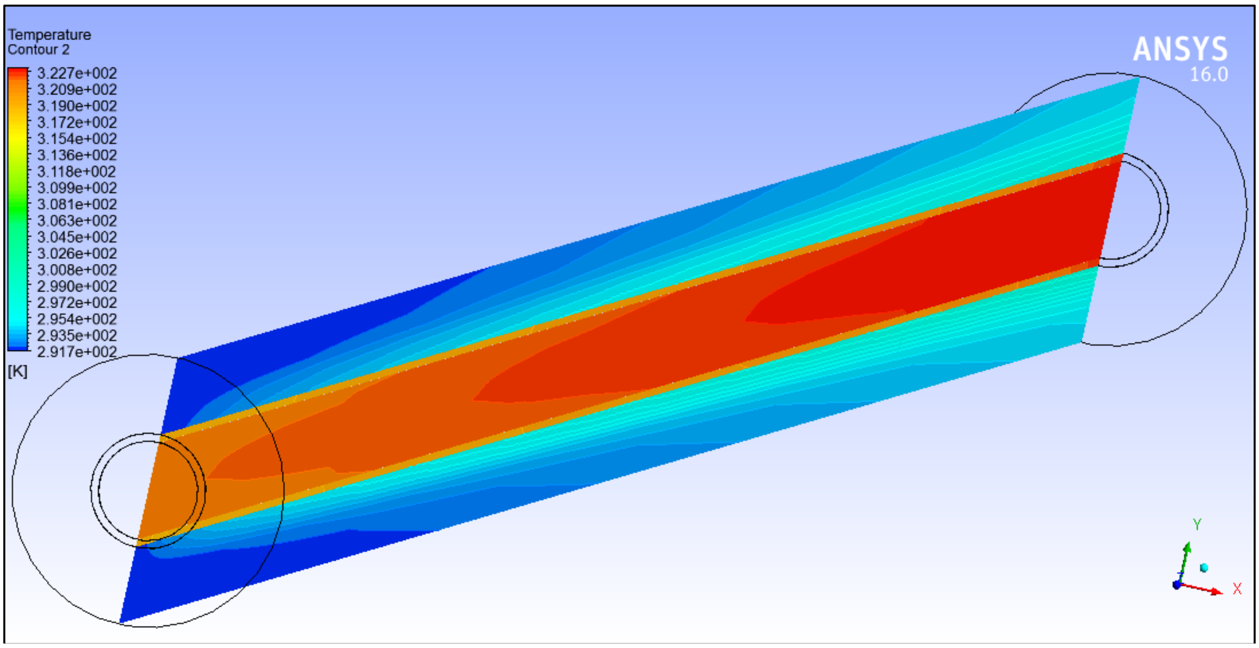

Figure (10): Temperature contours in (K) at (Z-axis) along the test section for Nano-fluid [2 % Al_2O_3].

Table (1): The Physical properties of the nanoparticles for (Al_2O_3) Nano-fluid.

Particle	Morphology	Color	Mean Diameter (nm)	Density (Kg/m^3)	Thermal Conductivity (W/m.c)	Specific Heat (J/Kg.c)
Al_2O_3	spherical	White powder	20	3970	40	765

Table (2): The (k-ε) model constants values.

$C_{1\varepsilon}$	$C_{2\varepsilon}$	C_{μ}	σ_k	σ_ε
1.44	**1.92**	**0.09**	**1**	**1.3**

Table (3): Details of numerical conditions.

ANSYS FLUENT (16)	
Inner diameter of inner tube	(19) mm
Thickness of inner tube	(1.5) mm
Inner diameter of shell	(52) mm
Dimensional	3D
Number of grid generation (nodes)	(124827)
Number of grid generation (element)	(91068)
Turbulence modeling	k–ε model
Outer fluid	Water
Interio fluid	AL_2O_3/Water
Pressure outlet	(P_o= 0)
Tube inlet temperature	(50) ^oC
Annulus inlet temperature	(18.6) ^oC
Velocity range of hot fluid	(from 0.176 to1.058) m/sec
Velocity of cold fluid	(0.529) m/sec

Table (4): The data of Nusselt numbers for (Al_2O_3) Nano-fluid and distilled water.

Discharge (L/min)	water	0.5-Al_2O_3	1-Al_2O_3	2-Al_2O_3
3	25.003	31.358	33.995	36.464
6	41.650	50.023	56.676	59.755
9	60.562	71.902	78.363	82.622
12	72.028	90.078	100.542	107.588
15	85.098	106.403	116.830	124.767
18	102.676	126.357	142.798	152.914

Table (5): The data of uncertainty error in Nusselt numbers for (Al_2O_3) Nano-fluid and distilled water.

Discharge (L/min)	water	0.5-Al_2O_3	1-Al_2O_3	2-Al_2O_3
3	2.339	2.434	2.535	2.550
6	0.691	0.647	0.722	0.732
9	0.338	0.314	0.343	0.346
12	0.200	0.192	0.206	0.225
15	0.136	0.130	0.139	0.143
18	0.106	0.098	0.109	0.117
Average	0.635	0.636	0.676	0.685

Nomenclature

Symbol	Description	Dimension
A	Surface area of the tube	m^2
C	Specific heat	kJ/kg.K
D	Diameter	m
G	Generation of turbulence kinetic energy due to the mean velocity gradients	$kg/m^3.s$
g	Ground accelerate	m/sec^2
h	Specific enthalpy	kJ/kg.K
h	Heat transfer coefficient	$W/m^2.K$
H	pressure head	m
k	Thermal conductivity	W/m. K
L	Length	m
$\dot{m}$	Mass flow rate	kg/s
m	Mass	kg
Nu	Nusselt number	---

P	Pressure	N/m^2
Q	Total heat power	W
Re	Reynolds number	---
S	modulus of the mean rate -of-strain tensor	---
T	Temperature	C^o
u, v, w	Velocity component in Cartesian coordinate	m/s
X,Y,Z	Cartesian coordinate	m

Greek Symbols

Symbol	Description	Dimension
φ	volume concentration of nanoparticles	---
γ	Crystalline phase	---
∂	Partial differential operation	---
μ	Dynamic viscosity	kg/m.sec
ε	Turbulence eddy dissipation rate	m^2/sec^3
κ	Turbulent kinetic energy	m^2/s^2
ρ	Density	kg/m^3
Δ	Difference between two value	---
∇	Represents the partial derivative of a quantity with respect to all directions in the chosen coordinate system	---
f	Friction factor	---

Subscripts

Symbol	Meaning
b	bulk
bf	Base fluid
e	Entrance
i, j, k	The three coordinate direction
i	Inlet, inner
nf	Nano-fluid
o	Outlet
s	Surface
t	Turbulent
W	Water

Abbreviation

Symbol	Description
CFD	Computational fluid dynamic
FLUENT	Fluid And Heat Transfer Code
ANSYS	Analysis System
3D	Three Dimension

References

1) Chol, S., Enhancing thermal conductivity of fluids with nanoparticles. ASME-Publications-Fed, 1995. 231: pp. 99-106.
2) Pak, B.C.C., Young I, Hydrodynamic and heat transfer study of dispersed fluids with submicron metallic oxide particles. Experimental Heat Transfer an International Journal, 1998. 11(2): pp. 151-170.
3) Fotukian, S.E., M Nasr, Experimental investigation of turbulent convective heat transfer of dilute γ-Al 2 O 3/water Nano-fluid inside a circular tube. International Journal of Heat and Fluid Flow, 2010. 31(4): pp. 606-612.
4) Vasu, V.K., K Rama Kumar, ACS, Analytical prediction of forced convective heat transfer of fluids embedded with nanostructured materials (Nano-fluids). Pramana, 2007. 69(3): pp. 411-421.
5) Wongcharee, K.E.-a., Smith, Heat transfer enhancement by using CuO/water Nano-fluid in corrugated tube equipped with twisted tape. International Communications in Heat and Mass Transfer, 2012. 39(2): pp. 251-257.
6) Khalifa, A.J.N.B., Mohammed A, Effect of Volume Fraction of γ-Al2O3 Nano-fluid on Heat Transfer Enhancement in a Concentric Tube Heat Exchanger. Heat Transfer Engineering, 2015. 36(16): pp. 1387-1396.
7) Nguyen, C.T.R., Gilles Gauthier, Christian Galanis, Nicolas, Heat transfer enhancement using Al2O3–water Nano-fluid for an electronic liquid cooling system. Applied Thermal Engineering, 2007. 27(8): pp. 1501-1506.
8) Vajjha, R.S.D., Debendra K Kulkarni, Devdatta P, Development of new correlations for convective heat transfer and friction factor in turbulent regime for Nano-fluid s. International Journal of Heat and Mass Transfer, 2010. 53(21): pp. 4607-4618.
9) Maddah, H.A., Reza Farokhi, Morshed Jahanizadeh, Shabnam Ashtary, Khatere, Effect of twisted-tape turbulators and Nano-fluid on heat transfer in a double pipe heat exchanger. Journal of Engineering, 2014.
10) Sivashanmugam, P., Application of Nano-fluid s in heat transfer. 2012: INTECH Open Access Publisher.
11) Xuan, Y.L., Qiang, Investigation on convective heat transfer and flow features of Nano-fluid s. Journal of Heat transfer, 2003. 125(1): pp. 151-155.
12) Frank M. White, Fluid Mechanics. Fourth ed., MacGraw-Hill books, 2001.
13) Pandey, S.D.N., VK, Experimental analysis of heat transfer and friction factor of Nano-fluid as a coolant in a corrugated plate heat exchanger. Experimental Thermal and Fluid Science, 2012. 38: pp. 248-256.
14) Wendt, J., Computational fluid dynamics: an introduction. Thired ed. 2008: Springer Science & Business Media.
15) Shih, T.-H., et al., A new k-ϵ eddy viscosity model for high Reynolds number turbulent flows. Computers & Fluids, 1995. 24(3): pp. 227-238.
16) Mahmoud, M.S., Theoretical Study Of Heat Transfer In Circular Holes For Turbine Blade. International Journal of Scientific & Engineering Research, 2013 4(2).